NUMERICAL MODELING OF ELASTO-VISCOPLASTIC CHABOCHE CONSTITUTIVE EQUATIONS USING MSC.MARC

ANDRZEJ AMBROZIAK

Department of Structural Mechanics,
Faculty of Civil and Environmental Engineering,
Gdansk University of Technology,
Narutowicza 11/12, 80-952 Gdansk, Poland
ambrozan@pg.gda.pl

(Received 22 October 2004; revised manuscript received 17 January 2005)

Abstract: The aim of the present paper is to propose a special kind of finite element procedure for dynamic and static analysis of civil engineering structures (*e.g.* trusses, beams, shells and spatial structures) including elasto-viscoplastic models. The Chaboche model with damage has been chosen from the wide range of available elasto-viscoplastic constitutive models for numerical calculations. The main advantage of the presented approach is the possibility of interference in subroutines and adjusting them to a particular problem (*e.g.* altering the form of constitutive equations). A user-defined UVSCPL subroutine has been proposed to introduce the elasto-viscoplastic model into the MSC.Marc system.

Keywords: elasto-viscoplastic constitutive models, damage, finite element method

1. Introduction

In materials where the viscous properties within the plastic range play an important role it is necessary to apply the elasto-viscoplastic constitutive relations. We can cite the following elasto-viscoplastic models for example: Perzyna [1], Chaboche [2], Aubertin [3], Lehmann-Imatani [4], Miller [5], Bodner-Partom [6], Krempl [7], Tanimura [8], Krieg-Swearengen-Jones [9], Walker [10], Korhonen-Hannjula-Li [11], Freed-Virrilli [12]. A detailed description of these models can be found in paper [13]. Their relatively large number shows that they are not universal and can be applied only under certain conditions or for a limited range of materials. From the wide range of available elasto-viscoplastic laws, the Chaboche model with damage has been selected in the present paper. This constitutive model is suitable for analysis of isotropic materials (mainly metals at high temperatures) in the range of small inelastic strains.

2. Description of the applied programs

Two computer programs have been applied in the present work. One has been a self-made FORTRAN code (OFC) for elasto-viscoplastic truss analysis. The theoretical description, FEM coding, details and application limits of this code are discussed in [14]. The other is the MSC.Marc system developed by MSC Software, a multipurpose finite element program for advanced engineering simulations. A great advantage of this system is the possibility to apply over 100 user-subroutines, which can be modified by the user. The standard MSC.Marc system does not support the Chaboche model with the damage concept proposed by Lemaitre (see *e.g.* [15]). Therefore, a user-defined UVSCPL subroutine [16] has been used to introduce the Chaboche model with continuous damage into the MSC.Marc system.

3. The Chaboche model

3.1. Basic equations of the Chaboche model with damage

In the first step, we assume an additive decomposition of the strain rates into the elastic $\dot{\boldsymbol{\varepsilon}}^E$ and inelastic $\dot{\boldsymbol{\varepsilon}}^I$ rate parts in the following form:

$$\dot{\boldsymbol{\varepsilon}} = \dot{\boldsymbol{\varepsilon}}^E + \dot{\boldsymbol{\varepsilon}}^I, \tag{1}$$

so that it is necessary to assume small strains. The relation between the stress and strain rates can be described for an isotropic material as:

$$\dot{\boldsymbol{\sigma}} = (1-D)\,\mathbf{B} : \dot{\boldsymbol{\varepsilon}}^E = \mathbf{B}^* : \left(\dot{\boldsymbol{\varepsilon}} - \dot{\boldsymbol{\varepsilon}}^I\right), \tag{2}$$

where $\mathbf{B}$ is the tensor of elastic modules.

In the Chaboche model, the inelastic strain rate has the form of:

$$\dot{\boldsymbol{\varepsilon}}^I = \frac{3}{2}\dot{p}\frac{\mathbf{S}' - \mathbf{X}'}{J(\mathbf{S}' - \mathbf{X}')}, \tag{3}$$

where $\dot{p}$, $\mathbf{S}'$ and $\mathbf{X}'$ are the rate of the equivalent plastic strain (the dots denote differentiation with respect to time) and the deviatoric parts of stress and back stress tensors, respectively. The $J(\mathbf{a})$ invariant is defined by the following equation:

$$J(\mathbf{a}) = \sqrt{\frac{3}{2}\mathbf{a} : \mathbf{a}} = \sqrt{\frac{3}{2}a^{ij}a_{ij}}. \tag{4}$$

We will consider the isotropic damage expressed by the scalar parameter $0 \le D \le 1$. The $\dot{p}$ rate in the Chaboche model with damage is defined in [15] as:

$$\dot{p} = \left\langle \frac{\frac{J(\mathbf{S}'-\mathbf{X}')}{1-D} - R - k}{K} \right\rangle^n, \tag{5}$$

where k, D and K, n are the initial yield stress, the damage parameter and material parameters, respectively. The angle bracket $\langle x \rangle$ has the following form:

$$\langle x \rangle = \frac{1}{2}(x + |x|) \tag{6}$$

and is called the McCauley bracket.

The isotropic hardening, R, and kinematic hardening, $\mathbf{X}$, are defined by the following expressions:

$$\dot{R} = b(R_1 - R)\dot{p}, \tag{7}$$

$$\dot{\mathbf{X}} = \frac{2}{3} a \dot{\boldsymbol{\varepsilon}}^I - c\mathbf{X}\dot{p}, \tag{8}$$

where a, c, b and R_1 are material parameters.

According to the damage model proposed by Kachanov [17], the damage evolution D used in Equation (5) is expressed by the following equation (see [15]):

$$\dot{D} = \left(-\frac{Y}{S}\right)^s \dot{p}, \tag{9}$$

where S, s are the material parameters of the damage and the $-Y$ function is given as:

$$-Y = \frac{1}{2(1-D)^2 E}\left(\frac{2}{3}(1+\nu)\boldsymbol{\sigma}_{eq}^2 + 3(1-2\nu)\boldsymbol{\sigma}_H^2\right), \tag{10}$$

where E is Young's modulus, ν is Poisson's ratio, and $\boldsymbol{\sigma}_{eq}$ and $\boldsymbol{\sigma}_H$ are the Huber-Misses equivalent stress and hydrostatic stress.

In the case of an uniaxial tension or compression state, the inelastic strain rate can be written as:

$$\dot{\boldsymbol{\varepsilon}}^I = \dot{p}\,\mathrm{sign}(\boldsymbol{\sigma} - X) = \left\langle \frac{\frac{|\boldsymbol{\sigma}-X|}{1-D} - R - k}{K} \right\rangle^n \mathrm{sign}(\boldsymbol{\sigma} - X) \tag{11}$$

while kinematic hardening has a simple form, [2]:

$$\dot{X} = a\dot{\boldsymbol{\varepsilon}}^I - cX|\dot{\boldsymbol{\varepsilon}}^I|. \tag{12}$$

It is worth noting that the stress tensor, $\mathbf{S}$, has one non-vanishing component, $\boldsymbol{\sigma}$, while the $\mathbf{S}'$ and $\mathbf{X}'$ tensors have three non-zero components:

$$\mathbf{S} = \begin{bmatrix} \boldsymbol{\sigma} & 0 & 0 \\ 0 & 0 & 0 \\ 0 & 0 & 0 \end{bmatrix}, \quad \mathbf{S}' = \begin{bmatrix} \frac{2}{3}\boldsymbol{\sigma} & 0 & 0 \\ 0 & -\frac{1}{3}\boldsymbol{\sigma} & 0 \\ 0 & 0 & -\frac{1}{3}\boldsymbol{\sigma} \end{bmatrix}, \quad \mathbf{X}' = \begin{bmatrix} \frac{2}{3}X & 0 & 0 \\ 0 & -\frac{1}{3}X & 0 \\ 0 & 0 & -\frac{1}{3}X \end{bmatrix}. \tag{13}$$

3.2. UVSCPL – the calculation algorithm

The UVSCPL [16] routine allows very general material laws to be entered into MSC.Marc. This user subroutine has been used in the present work for computing the inelastic strain increment for the elastic-viscoplastic Chaboche material model. In general, the inelastic strain rate and the stress increment must be defined in the procedure. The main part of the algorithm used in the computation is presented in Figure 1 (where j is the number of time steps). As in expressions for step j, the components from the same step are used and iterations are necessary at each step.

Additionally, the PLOTV [16] routine has been used to visualize the evolution of the damage parameter. In this procedure, it is simple to define the variable to be plotted and written to the post file.

4. Numerical examples

Numerical calculations have been performed for simple solid (Figure 2) and truss (Figure 3) structures. Such tests are usually performed in a laboratory during

$$[\text{step 1}] \rightarrow \begin{bmatrix} \Delta\mathbf{X} = \dfrac{\Delta t}{2}\left(\dot{\mathbf{X}}_{j-1} + \dot{\mathbf{X}}_j\right), & \mathbf{X}_j = \mathbf{X}_{j-1} + \Delta\mathbf{X} \\ \Delta R = \dfrac{\Delta t}{2}\left(\dot{R}_{j-1} + \dot{R}_j\right), & R_j = R_{j-1} + \Delta R \\ \Delta D = \dfrac{\Delta t}{2}\left(\dot{D}_{j-1} + \dot{D}_j\right), & D_j = D_{j-1} + \Delta D \end{bmatrix}$$

$$[\text{step 2}] \rightarrow \left[\, \mathbf{S}'_j,\ \mathbf{X}'_j,\ J(\mathbf{S}'_j - \mathbf{X}'_j),\ J(\mathbf{S}'_j),\ \mathrm{tr}(\mathbf{S}_j) \,\right]$$

$$[\text{step 3}] \rightarrow \left[\, \dot{p}_j = \left\langle \frac{J(\mathbf{S}'_j - \mathbf{X}'_j)/(1 - D_j) - R_j - k}{K} \right\rangle^n \,\right]$$

$$[\text{step 4}] \rightarrow \left[\, \dot{\boldsymbol{\varepsilon}}^I_j = \frac{3}{2}\dot{p}_j \frac{\mathbf{S}'_j - \mathbf{X}'_j}{J(\mathbf{S}'_j - \mathbf{X}'_j)} \,\right]$$

$$[\text{step 5}] \rightarrow \left[\, \dot{\mathbf{X}}_j = \frac{2}{3} a \dot{\boldsymbol{\varepsilon}}^I_j - c\mathbf{X}_j \dot{p}_j \,\right]$$

$$[\text{step 6}] \rightarrow \left[\, \dot{R}_j = b(R_1 - R_j)\dot{p}_j \,\right]$$

$$[\text{step 7}] \rightarrow \left[\, \dot{D}_j = \left(-\frac{Y}{S}\right)^s \dot{p}_j \,\right]$$

$$[\text{step 8}] \rightarrow \left[\, \mathbf{B}^*_j = (1 - D_j)\mathbf{B} \,\right]$$

$$[\text{step 9}] \rightarrow \left[\, \Delta\boldsymbol{\varepsilon}^I_j = \dot{\boldsymbol{\varepsilon}}^I_j \Delta t_j \,\right]$$

$$[\text{step 10}] \rightarrow \left[\, \Delta\mathbf{S}_j = \mathbf{B}^*_j(\Delta\boldsymbol{\varepsilon}_j - \Delta\boldsymbol{\varepsilon}^I_j) \,\right]$$

Figure 1. Flow graph of the UVSCPL subroutine

identification of the Chaboche model material parameters [18]. The identification's results can be immediately applied in 3D or 2D analysis, on the assumptions of small strains and isotropy of the material.

Three-dimensional eight-node isoparametric solid (Element 7, see [19]) and three-dimensional two-node straight truss (Element 9, see [19]) elements were applied in the MSC.Marc calculations. Trilinear interpolation functions were used in the former

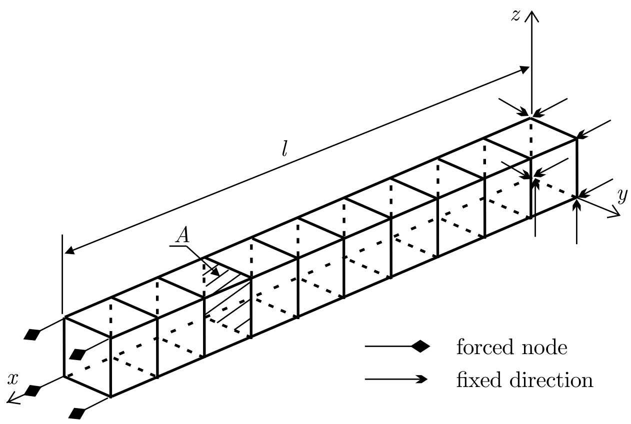

Figure 2. Geometry of the solid structure

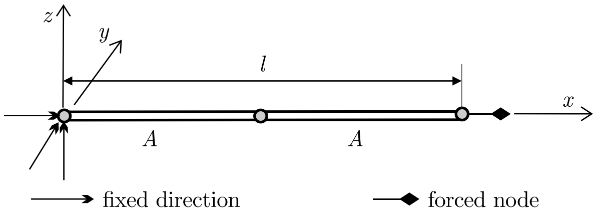

Figure 3. Geometry of the truss structure

and thus the strains tend to be constant throughout the element. Linear interpolation was used in the latter for coordinates and displacements. At the same time, only the straight two-nodes truss element with simple linear interpolation was used in the OFC program.

The geometrical parameters of $l = 1.0\,\mathrm{m}$ (length) and $A = 0.001\,\mathrm{m}^2$ (square cross section area for the truss and solid elements) were assumed. Due to the purely numerical character of the work the values of the material parameters were taken from the literature. The author is aware that sometimes different sets of parameters can be found in the literature for the same material under the same conditions due to the strong physical nonlinearity of the problem (see [20]). In practical applications such sets must be carefully verified.

4.1. Example 1 (without damage)

The following material parameters were assumed in the first step of the numerical calculations (INCO718 nickel-based alloy at 650°C from [21]): $E = 159.0\,\mathrm{GPa}$, $\nu = 0.3$, $k = 514.21\,\mathrm{MPa}$, $b = 60.0$, $R_1 = -194.39\,\mathrm{MPa}$, $a = 170.0\,\mathrm{GPa}$, $c = 500.0$, $n = 4.0$, $K = 1023.5$ $(\mathrm{MPa \cdot s})^{1/n}$, $S = 0.0\,\mathrm{MPa}$, $s = 0.0$.

The stress versus strain diagrams for various strain rates ($10^{-7} \le \dot{\varepsilon} \le 10^{-1}\,\mathrm{s}^{-1}$) are presented in Figure 4. The result of the creep test is shown in Figure 5 (the constant stress condition applied at the level of $\boldsymbol{\sigma} = 1000\,\mathrm{MPa}$). There is no difference

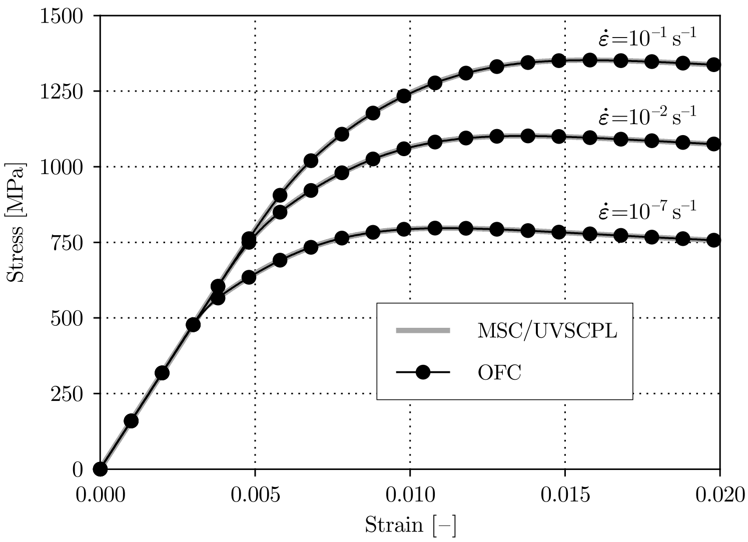

Figure 4. Constant stress rate tests

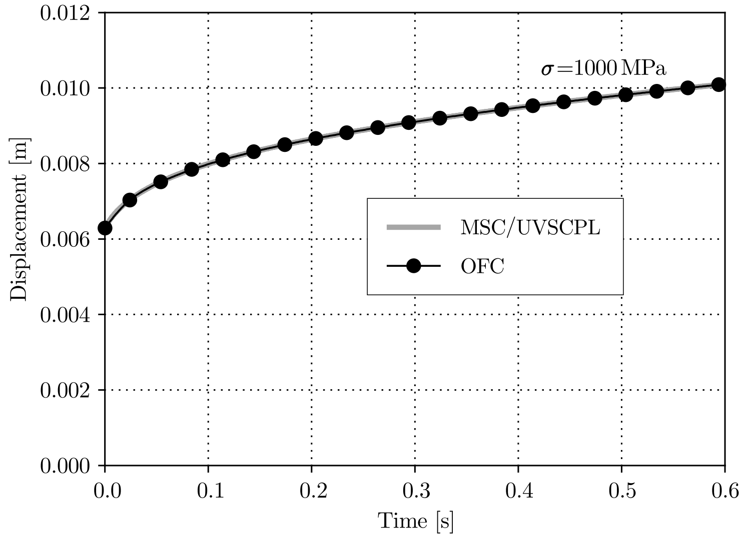

Figure 5. Creep test

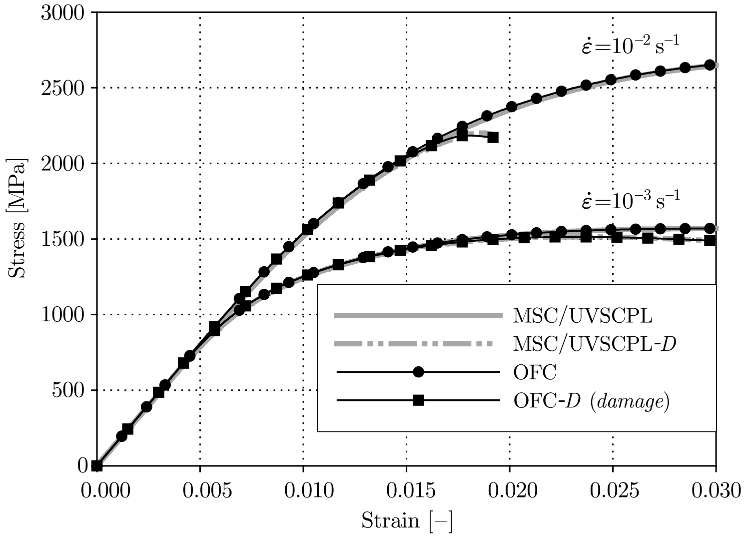

Figure 6. Constant stress rate tests

between the results obtained from the two computer programs and the types of finite elements used in the numerical calculations.

4.2. Example 2 (with damage)

The following material parameters were taken for the Chaboche model coupled to damage (INCO718 alloy at 627°C from [18]): $E=162.0\,\mathrm{GPa}$, $\nu=0.3$, $k=501.0\,\mathrm{MPa}$, $b=15.0$, $R_1=-165.4\,\mathrm{MPa}$, $a=80.0\,\mathrm{GPa}$, $c=200.0$, $n=2.4$, $K=12790.0$ $(\mathrm{MPa\cdot s})^{1/n}$, $S=4.48\,\mathrm{MPa}$, $s=3.0$. The reference calculations for this case were conducted with damage constants $S=0.0\,\mathrm{MPa}$, $s=0.0$.

The stress versus strain graphs for the two strain rates, $\dot{\varepsilon}=0.001\,\mathrm{s}^{-1}$ and $\dot{\varepsilon}=0.01\,\mathrm{s}^{-1}$, are shown in Figure 6, where the influence of damage is apparent. In

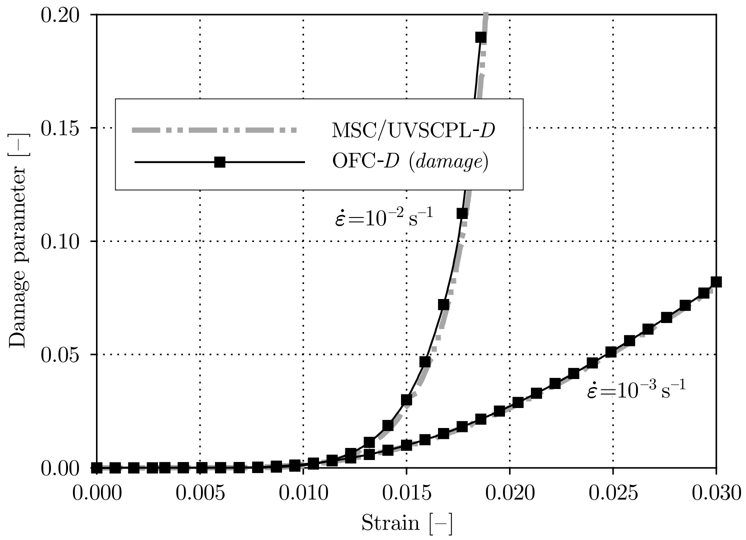

Figure 7. Change of the damage parameter in the constant stress rate tests

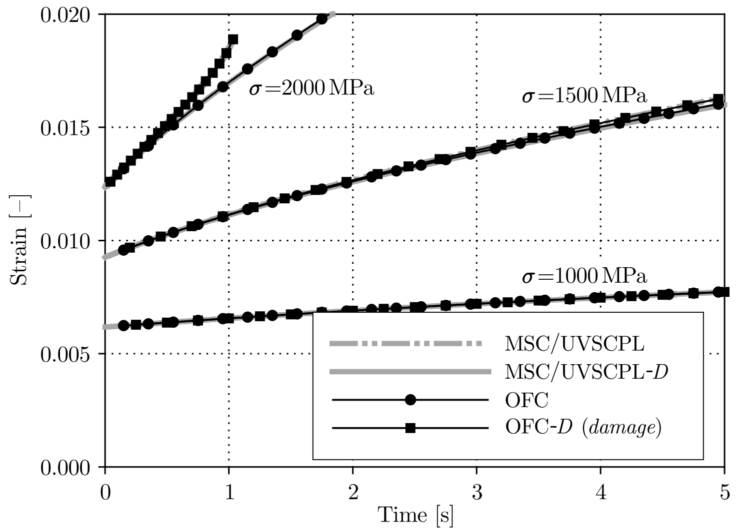

Figure 8. Creep test

the analysed range of strain and stress, damage of the structure and a break in the numerical calculations was observed in the case of the $\dot{\varepsilon}=0.01\mathrm{s}^{-1}$ computation. The evolution of the damage parameter is given in Figure 7; for the $\dot{\varepsilon}=0.01\mathrm{s}^{-1}$ calculation damage exceeds the value limit. The simulations of creep tests are presented in Figures 8 and 9 and for the stress values of $\boldsymbol{\sigma}=1000\mathrm{MPa}$ and $\boldsymbol{\sigma}=1500\mathrm{MPa}$. In this case, the damage has great influence for $\boldsymbol{\sigma}=2000\mathrm{MPa}$. Finally, a diagram of the cyclic load test for $\dot{\varepsilon}=0.001\mathrm{s}^{-1}$ is shown in Figure 10. The cyclic test was carried out in the range of $\varepsilon=0.03$. Like in the first example, there is no significant difference between the results obtained from the two computer programs. It is worth pointing out the additive character of the damage parameter. Its value increases at each successive step, expect for the elastic range of deformation, where its value is constant due to

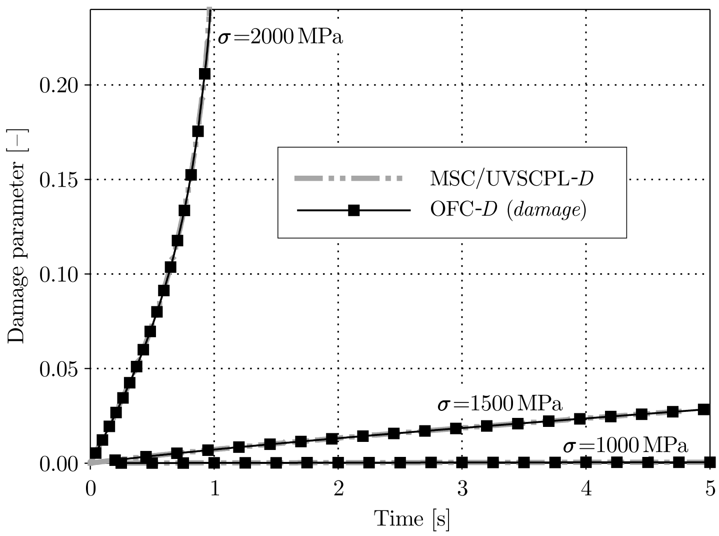

Figure 9. Change of the damage parameter in the creep tests

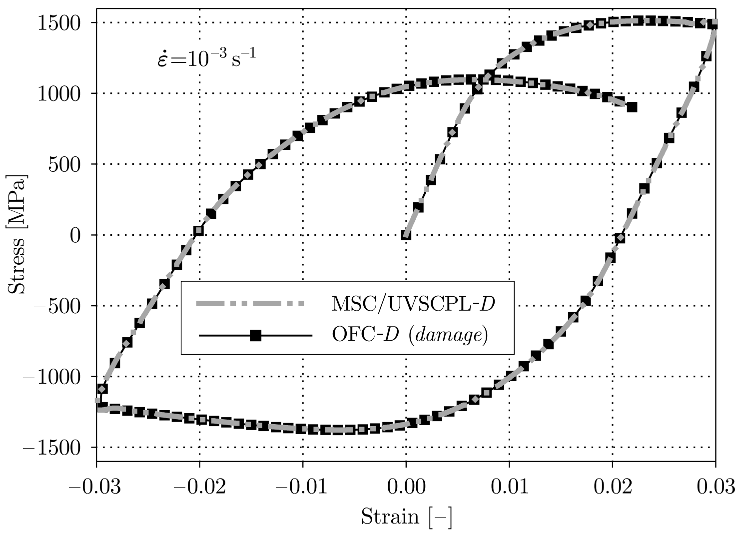

Figure 10. Cyclic test

the lack of inelastic effects (see Figures 11 and 12). The failure of the specimen after a single cycle of loading is attributable to the relatively high strain rate. An error in the determination of material constants is another possible explanation. For example, the material parameter K has a very high value compared to other references in the literature (*cf. e.g.* [22, 23]).

5. Conclusions

The following conclusion and remarks may now be formulated:

(1) Thanks to the possibility of including user's constitutive model subroutines into the MSC.Marc system, the Chaboche model with damage can be directly applied in calculations.

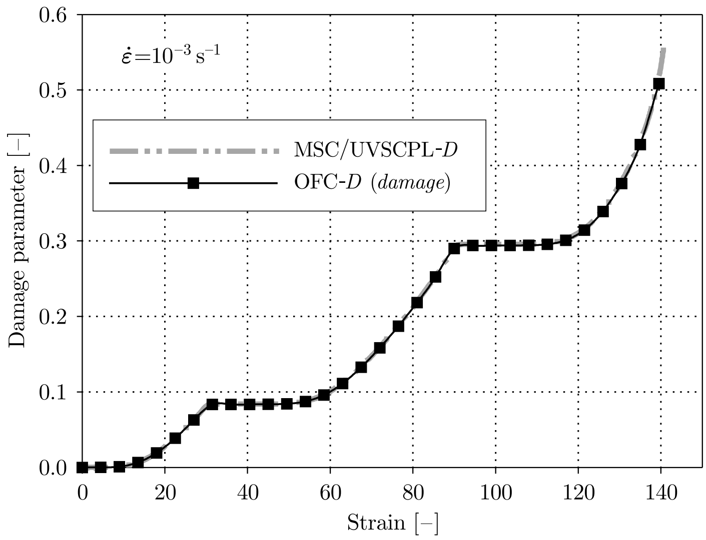

Figure 11. Change of the damage parameter of the cyclic test in the time domain

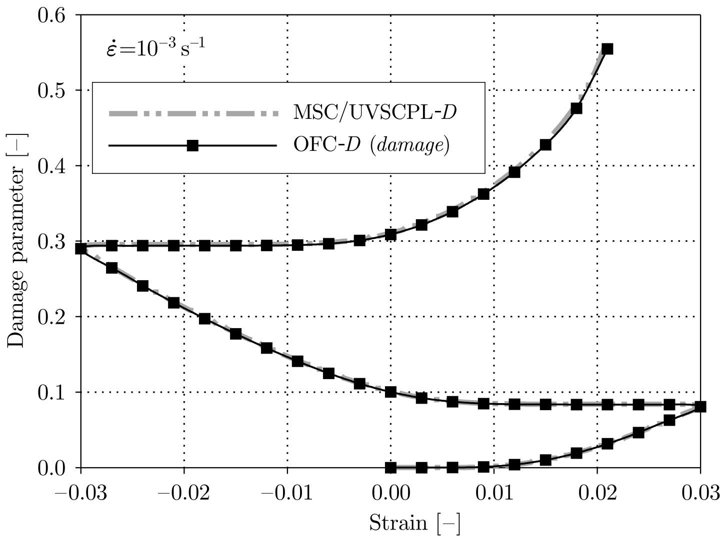

Figure 12. Change of the damage parameter of the cyclic test in the strain domain

(2) A non-linear analysis of simple solid and truss structures with elastic-viscoplastic physical equations for the Chaboche model has been successfully carried out.

(3) The MSC.Marc and OFC programs respond almost identically in all the calculated test variants.

(4) The obtained results require a revision for more complex structures, types of analysis and kinds of load. Especially the influence of layering in the shell elements should be investigated.

(5) Further research should focus on the development of the UVSCPL routine with an emphasized influence of temperature.

Acknowledgements

The research was performed within the Polonium 2005 Polish-French cooperation program administrated by KBN and ÉGIDE (KBN 5598.II/2004/2005).

Calculations presented in the paper were performed at the Academic Computer Centre in Gdansk (TASK).

The study was supported by the European Community under the FP5 Programme, key-action "City of Tomorrow and Cultural Heritage" (Contract No. EVK4-CT-2002-80005). This support is acknowledged with gratitude.

References

[1] Perzyna P 1978 *Thermodynamics of Elastic Materials*, PWN, Warsaw (in Polish)

[2] Chaboche J L 1989 *Int. J. Plasticity* **5** 247

[3] Aubertin M, Gill D E and Landanyi B 1991 *Mechanics of Materials* **11** 63

[4] Lehmann T 1984 *Cours and Lectures*, Vol. 281, Springer, Wien – New York

[5] Miller A 1976 *J. Engng. Mat. and Technol., ASME* **98** 97; *ibid.* 106

[6] Bodner S R and Partom Y 1975 *J. Appl. Mech., ASME* **42** 385

[7] Krempl E, McMahon J J and Yao D 1984 *Mechanics of Material* **5** 35

[8] Tanimura S 1979 *J. Int. Engng. Sci.* **17** 997

[9] Krieg R D, Swearengen J C and Jones W B 1987 *Unified Constitutive Equations for Creep and Plasticity* (Miller K, Ed.), Elsevier, pp. 245–271

[10] Freed A D and Walker K P 1989 *The Winter Annual Meeting of the ASME* (Hui D and Kozik T J, Eds.), San Francisco, pp. 10–15

[11] Korhonen M A, Hannjula S P and Li C Y 1987 *Unified Constitutive Equations for Creep and Plasticity* (Miller K, Ed.), Elsevier, pp. 89–138

[12] Freed A D and Virrilli M J 1988 *Proc. of the MECAMAT*, Besançon, Vol. I, pp. 27–39

[13] Woznica K 1998 *Dynamique des structures élasto-viscoplastique*, Cahiers de Mechanique, Lille

[14] Kłosowski P and Woznica K 2000 *Machine Dynamics Problems* **24** (3) 33

[15] Lemaitre J 1985 *J. Engng. Mat. and Technol.* **107** 83

[16] *Users handbook: MSC.Marc*, Volume D: User Subroutines and Special Routines, Version 2003. MSC.Software Corporation 2003

[17] Kachanov L M 1958 *TVZ Akad. Nauk. S.S.R. Otd. Tech. Nauk.* **8** 26

[18] Ammar G and Dufailly J 1993 *European J. Mech., A/Solids* **12** 197

[19] *Users handbook: MSC.Marc*, Volume B: Element Library, Version 2003. MSC.Software Corporation 2003

[20] Kłosowski P, Schmidt R and Weichert D 1997 *Engineering Translations* **45** 91

[21] Golinval J C 1989 *Calcul par éléments finis de structures élasto-viscoplastiques somies à des chargements cycliques à haute temperature*, Collection des publications de la Faculté des Sciences Appliques, Universiteté de Liège, No. 126b

[22] Efits J, Abdel Kader M S and Jones D I 1989 *Int. J. Plasticity* **6** 1

[23] Lewandowski M S and Overfelt R A 1999 *Acta Mater.* **47** 4695